Microfluidic preparation of alginate microparticles for targeted delivery

Christian Leonardo Riera Orozco

christianorozco@tecnico.ulisboa.pt

Departamento de Engenharia Química, Intituto Superior Técnico - Lisbon, Portugal
Laboratory of Biomimetic Engineering, University of Chemistry and Technology - Prague, Czech Republic

14 December 2020

Abstract

Whether termed micro-total analysis systems, lab-on-a-chip, or microfluidic devices, the technologies that define the field of microfluidics have shown great promise for overcoming many challenges in environmental, clinical, chemical and biological analyses.The objective of this work was to produce microparticles of alginate containing iron oxide nanoparticles that increase the ease of manipulation of the particles. After, the particles surface was modified to give copolymer properties to the particles and thus be able to assign properties necessary for each situation or to transport substances through targeted delivery. The size of each particle was measured and compared to obtain a mathematical model that can predict the particles sizes for different flow rates.A flow focusing cross junction microfluidics reactor was designed in PDMS which can control the size of microparticles by adjusting the flow rate of inlets.This approach offers a potentially lower cost, adjustable process for making microparticle compared to other more traditional polymerization approaches.Computational models can also help to produce pressure droplet correlations. In this work, COMSOL Multiphysics was used to contribute to the determination of how the fluid behave in the junction and how the particles is produced.

Keywords : Microfluidics, alginate, undecanol, targeted delivery, COMSOL multiphysics

1. Introduction

Throughout the last century miniaturization has played a crucial role in modern technology and revolutionized society. Great advances has been made in both technology (micro- and nanotechnology),but also within the fields of chemistry and biology, where improvements in optical systems has opened a world of new possibilities.

One of these improvement has been in the field of microfluidics, the science of manipulating and controlling fluids, usually in the range of microliters(10^{-6}) to picoliters (10^{-12}), in networks of channels with dimensions from tens to hundreds of micrometers [1]. At this scale, researchers can take advantage of the scaling of many physical laws and employ, for example, rapid diffusion, laminar flows, dean flow, rapid thermal transport, and take advantage of the large surface area relative to the volume [2].

So microfluidics seems almost too good to be true: it offers so many advantages and so few disadvantages (at least in its major applications in analysis). In fact, concerning the time and circumstances required for microfluidics to develop into a major new technology are important not just for this field,but also for other new technologies struggling to make it into the big time. Empowered by the versa-tile microfabrication technologies that have stemmed from the technologies used for microelectronics and microelectromechanical systems (MEMS), microfluidics offers salient advantages over conventional platforms, such as high resolution and sensitivity in separation and detection, lower cost for fabrication than laboratorial or industrial devices, low sample consumption and low waste, short time for analysis,and small device footprint.

The development of microfluidics has just begun. A number of factors suggest that there are many early stage applications of microsystems containing fluids, including the exploration of fluidic optics and cells, the development of new types of organic synthesis in small-channel systems, the continuing development of technologies based on large arrays of detectors and on high-throughput screening, the fabrication of microrobotic systems using hydraulic systems based on microfluidics, other fluidic versions of MEMS, and work on biomimetic systems with microfluidic components [3].

2. Methods

2.1. Chip production

There are two processes for producing PDMS microchips, each with its own advantages and disadvantages.Using plasma surface activation for bonding the microchips parts or heating attachment, coming in contact the surfaces when they are not completely solid and taking advantage of the curing process. The first process allows a great bonding of the microchip parts. However, the hydrophilic character of the microchip after plasma treatment can be a problem. On the other hand, heat

attachment allows to produce microchips in a short time but can produce air bubbles inside the microchip.

The PDMS microchips were fabricated by pouring a degassed mixture of Sylgard 184 silicone elastomer and curing agent onto master microchip mold on silicon wafer with positive relief for microchip top as well as a blank Petri dish for bottom. For each process different base/curing agent ratio were used (Table 1)

Table 1: Ratio of the mixture between elastomer base and curing agent for heat attachment and surface activation process.

	Ratio base/curing agent	
	Upper	Bottom
Surface activation	10:1	10:1
Heat attachment	5:1	14:1

After degassed in a desiccator, the wafer and Petri dish with polymer was cured in an oven, at 70°C, for 2 hours for surface activation and around 20 min for heat attachment, until the microchip parts achieve enough hardness to preserve the pattern.

2.1.1. Pattern clearing

The PDMS microchip was cut with a curved razor blade, gently lifting the excised pieces from the master mold, inserting microwires into designated inlets and outlet channels and traces of dust were removed from the both parts of the microchip by scotch tape.

2.1.2. Parts assembly

The last part of the microchip production is assembling the parts. As mentioned before, plasma can be used for this. Plasma, as the fourth state of matter, is generated by heating or subjecting a neutral gas to electromagnetic fields. It is composed of a high concentration of reactive species, including ions, electrons, neutrons, excited molecules, free radicals, metastable particles and photons that are capable of inducing physical and chemical changes on polymeric surfaces. When an object undergoes a plasma bonding process, the surface energy is raised due to bombardment of charged particles of the plasma such as ionized atoms or molecules and electrons that react chemically with the surface by sputtering effect.

It was used Diener Zepto plasma system for the surface activation and defining the following parameters, the top part was sticked to the bottom part:

- Pressure - stable between 0,2 and 0,3 mbar;
- Power - 30%;

After 50 seconds under plasma surface activation the microchip was assembled and left 48 hours into the oven at 70°C for removing the hydrophilicity caused by the plasma.

For the preparation of these chips with heat attachment, the two parts of the chip are bonded when the surfaces are not completely solid so they can attach easily without using the plasma surface activation. After pattern clearing, the parts were assembled and left into the oven at 70°C for over 2h.

2.2. Iron oxide

For preparation of the solution of iron oxide, iron(III) chloride hexahydrate and iron(II) chloride tetrahydrate are diluted in water in the proportion 3:1,5:100 (w/w) and stirred for 10 min at 475 rpm. After slowly increasing of the temperature to 80°C during 10 minutes, it was added 20 ml of ammonium hidroxide and 10 ml after 1 hour. The solution continue stirring for 1h and then an 48 ml of aqueous solution of trisodium citrate dihydrate, 5:1 (w/w), is added to the previous solution and left stirring for 1h. Finally, this solution is dialized for 24 hours.

2.3. Preparation of dispersed phase solution

Iron oxide is embedded inside the alginate solution in order to separate these particles from the other substances, applying an external magnetic field. For this process, a solution of iron oxide and alginate 0,025% is prepared. The iron oxide used is the solution, diluted 1:2 (c= 5,62 mg/mL) and a solution of alginate 0,05% alginate prepared previously, diluting 0,5g of alginate in 10g of deionized water (Figure 1).

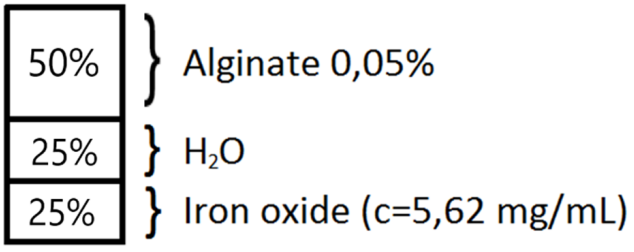

Figure 1: Percentage of iron oxide and alginate used for dispersed phase solution.

2.4. Preparation of continuous phase

Two continuous phases are prepared for this experiment, based on 1-undecanol. They are used in different moments of the microparticles productions.

- Couninuous phase 1, composed by 1-undecanol with surfactant ABIL Em 90 (5% w/w);
- Continuous phase 2, consists in 1-undecanol with surfactant ABIL Em 90 (5% w/w) and 2% of calcium iodide;

2.5. Fabrication of microparticles in the microfluidic device

The schematic representation of the microfluidic device is illustrated in Figure 2. The flow-focusing device consists of three inlets, one outlet, two junctions and ex-

panding chamber. The continuous phases fluids are injected into the other inlets 1 (continuous phase 1) and 2 (continuous phase 2) while dispersed phase fluid is injected into the inlet 3. The three fluids are inserted through syringes (Hamilton 0.25 ml, Hamilton 5 ml, and Hamilton 2.5 ml, respectively) connected by teflon capillaries (ID 0.8 mm, OD 1.6 mm) and attached to the linear pumps (neMESYS 290N, Cetoni) to provide constant flowrate of each phase. Continuous phase 1 fluid flowing from two opposite sides of the channel brakes the dispersed phase at the junction, which lead to generating droplets at the orifice channel, or the expanding chamber.

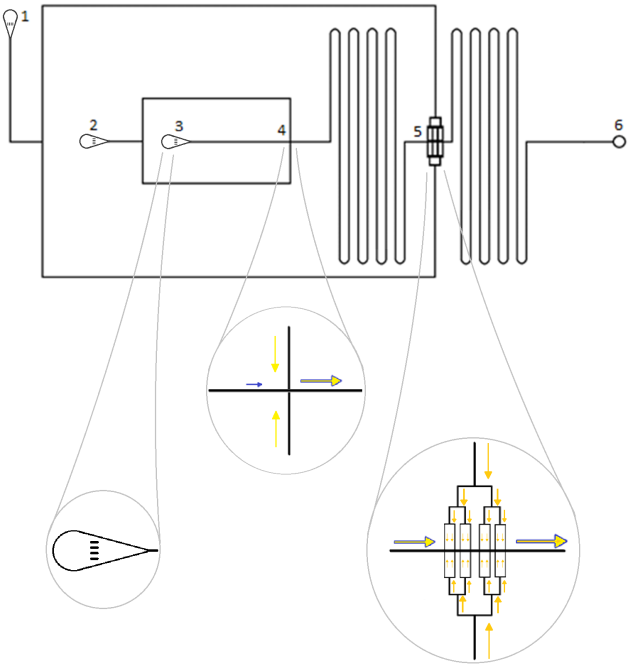

Figure 2: Microchip scheme: 1-input of oil with Ca+; 2- input of oil; 3 input of alginate solution; 4- mixture between oil and alginate; 5- solidification of microparticles by addition of oil with Ca+; 6- output of particles.

Initially, all capillaries were filled with an appropriate solution, to prevent the formation of bubbles inside the chip. For all experiments and the reliability of the results of each test, the device is continuously operated for 10 min with constant flow rate, and then the results of the experiments are recorded. The experiments are monitored by an inverted microscope. Continuous Phase I meets the dispersed and droplets are formed (see Figure 2-4). In the following wavy section of the microfluidic chip, water extraction for 1-undecanol occurs, leading to a reduction in the size of the aqueous droplets. Thereafter, the flow of calcium ions is introduced into the fluid flow as Phase II continuous (Figure 2-5). In the following wavy structure, the reticulation and gelation of alginate occurs, leading to the formation of solid alginate microparticles.

2.6. Particles modification

The last part of the process was to modify the particles so that they are ready for future use in target delivery.

2.6.1. Chitosan stabilization

Chitosan was used for creating complexes alginate-chitosan by electrostatic interaction between the anionic residues of alginate and a positively charged amino terminals of chitosan. In this way, the structure of the microparticles became more stable. After cleaning with pure 1-undecanol and later with water, the particles were decanted using a magnet, taking advantage of the magnetic properties of the iron oxide. Meanwhile, a 1% (w/w) chitosan solution was prepared into 1% (w/w) acetic acid solution. Finally, the particles were transferred to the chitosan solution and stirred for 24h.

2.6.2. Glutaraldehyde cross-linking

In order to provide copolymer properties, a cross-linking agent was added to the surface of the particles (Figure 3). After stabilizing the particles with chitosan, they were washed with PBS solution, transferred into 1 ml of glutaraldehyde solution (10% v/v) and incubated (Eppendorf ThermoMixer C) for 1 hour (25 °C, 1 000 rpm). Afterwards, the particles were washed three times with PBS solution.

A different cross-linker could be also used for the modification since it depends on which group is going to react during the bonding process. In this case, the hydroxyl groups of the glutaraldehyde are the responsible for the bonding.

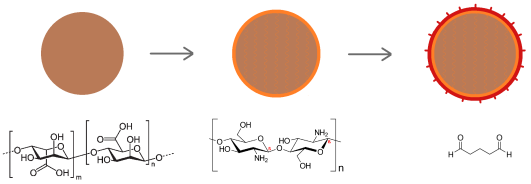

Figure 3: Modification process: Stabilizing the alginate microparticle shape with chitosan and cross-linking with glutaraldehyde as cross-linker

2.7. COMSOL Multiphysics simulation

In this study, the microfluidic chip designed above was modeled using the finite element method. The necessary procedures have been made to analyze the microfluidic chip designed using the COMSOL Multiphysics.

By using COMSOL Multiphysics tests and analyzes will be made. These analysis give the desired analysis and results to the user without producing the microchip. In the COMSOL Multiphysics program, it is possible to make many analyzes related to physics parameters.

This steps were followed in order to simulate microfluidics in COMSOL Multiphysics:

- Geometry modeling. According to the subject's shape and the condition of microfluidics, a model 2D of the flow focusing cross section in designed in Corel Draw and established in COMSOL;
- Physics settings. Physics menu contains two settings, which are subdomain settings and boundary settings. Subdomain settings is for setting each domain's material property, initial conditions etc. Boundary settings is for setting boundary conditions in two aspects. Firstly, it can set boundary conditions on the interface of different materials. Secondly, it can also set boundary conditions on the interface between material and the environment;
- Solving. COMSOL Multiphysics's solver can be selected for dealing with different problems. Users can either select the proper solver according to their problem or use the default setting. Refers to this thesis, the author use the default setting to solve the three heat transfer problems;

And the following input parameters specify the behavior of the dispersed phase in the continuous phase and the flow rate of each input, which are;

- Pressure input in the continuous phase microfluidic channel;
- Pressure input in the dispersed phase microfluidic channel ;
- Velocity inlet of the continuous phase to the microfluidic channel;
- Velocity inlet of the dispersed phase to the microfluidic channel;
- Surface tension of the continuous phase;
- Surface tension of the dispersed phase;

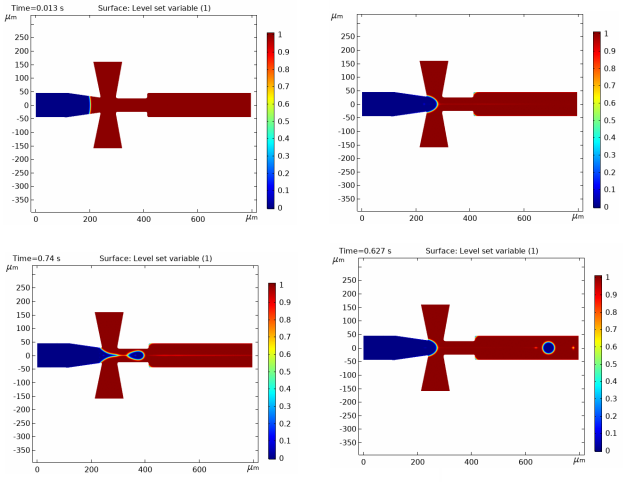

Figure 4: Simulation with COMSOL Multiphysics of a flow focusing cross-junction microfluidics with alginate solution as dispersed phase and 1-undecanol as continuous phase.

It is possible to compare the mathematical models with the results obtained in the experiment, regarding the flow of alginate and oil(Figure 4).

The cross-junction was simulated by COMSOL Multiphysics. At this point two liquids interact: the continuous phase, 1, in red and the dispersed phase, 2, in blue. Among them there is the oil-water interphase, which is important for the formation of particles.

3. Results and discussion

3.1. Dependence between drop size and flow rate

Figure 5 shows images taken from the monodispersed droplet formation experiments, with each image corresponding to different oil flow rate. In this assay, the total aqueous flow rate was fixed at 10 μl/h.

The particle diameter (d) was measured from the images using the imaging processing software QuickPHOTO MICRO 3.2. Particles produced with continuous flow rate of 60 and 110 μl/h are shown in Figure 5. It can be seen that the increase of oil flow reduced the drop size.

In shear driven flow, the capillary number is important for determining the size of the droplet after breakup. The capillary number, Ca=μu/σ, is defined as the ratio of shear stress exerted on the droplet and interfacial tension of the droplet, where μ is the dynamic viscosity of the oil phase,U the characteristic of the fluid and σ is the interfacial tension between water and oil interface.

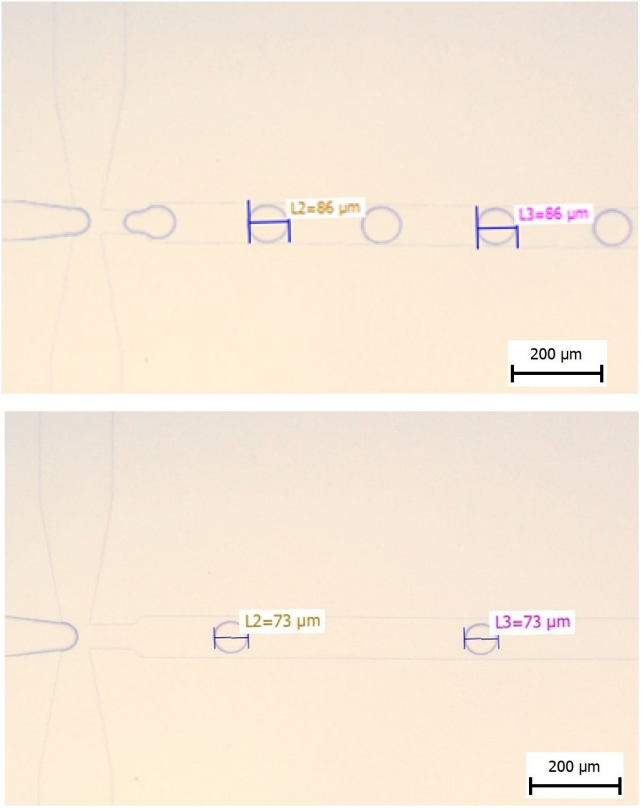

Figure 5: Images of droplet formation for different oil phase flow rates. The total aqueous phase was kept at 10 μl/h. While the oil assumes values of 60 μl/h (top left), 70 μl/h (top right) and 80 μl/h (bottom).

In this device, since droplet breakup occurs at the

orifice when the neck of the droplet becomes a singular point, where the cross-sectional area of the neck is small compared to the cross-sectional area of the channel, the shear rate generated by the oil phase can be approximated as the velocity of the oil flow divided by the width of the channel, since the dispersed phase flow rate is negligible compared to the oil phase.

In Figure 6, the drop size as a function of the flow rate shows the variation with a constant flow rate of the dispersed phase, in different assays . At the lowest flow rate ratios the drop sizes are nearly on the order of the flow-focusing orifice size, d/D≈1, which indicates the geometric control of drop size common to many microfluidic experiments.

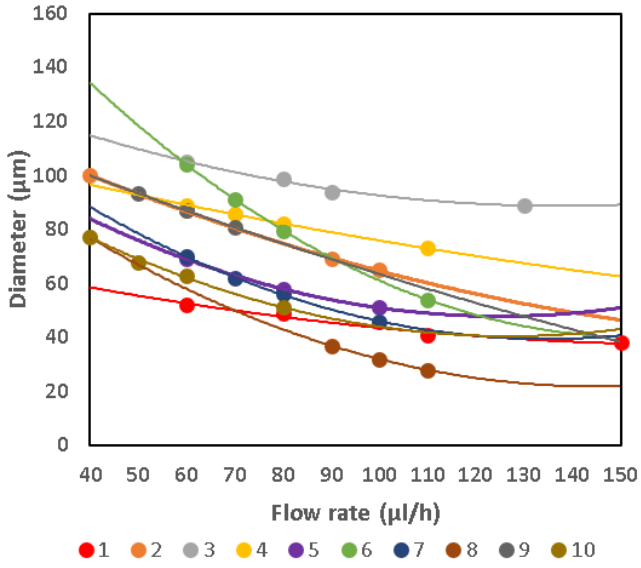

Figure 6: Droplet diameter versus flow rate of the oil, for a constant dispersed phase flow rate.

For each test, it was added a trend line that adjusted better to the points (Figure 6). In all cases, a quadratic function fit well, with a R^2 greater than 0,98. The decrease in particle diameter is between 4,8 and 14% for each increment of 10 μm in the continuous phase flow rate, depending on the initial flow rate of the continuous phase.

The quadratic functions are defined by $\mathbf{a}x^2+\mathbf{b}x+\mathbf{c}=0$ where each variable **a**, **b**, **c** have a different role in the standard form of the quadratic functions.

- The value of **a** changes the width of the opening of the parabola and that the sign of **a** determines whether the parabola opens upwards or downwards.
- The value of **b** moves the axis of symmetry of the parabola from side to side; increasing b will move the axis in the opposite direction.
- The value of **c** moves the vertex of the parabola up or down and **c** is always the value of the y-intercept.

In this experiment, the variable b and c is related to the particle size, which depends on the dispersed phase flow rate used for each assay. On the other hand, the variable a represents the variation of the particle size for different flow rates. It can be seen, that the value of a oscillates around the value of **a**≈ 0,0056 (Figure 7). That means that, knowing the size of some particles, specifically. With a couples of particles, **B** and **C**, with size **b1** and **c1**, produced with a oil flow rate **b2** and **c2**, respectively, is possible to obtain an estimated value of the particle diameter for each every oil flow rate.

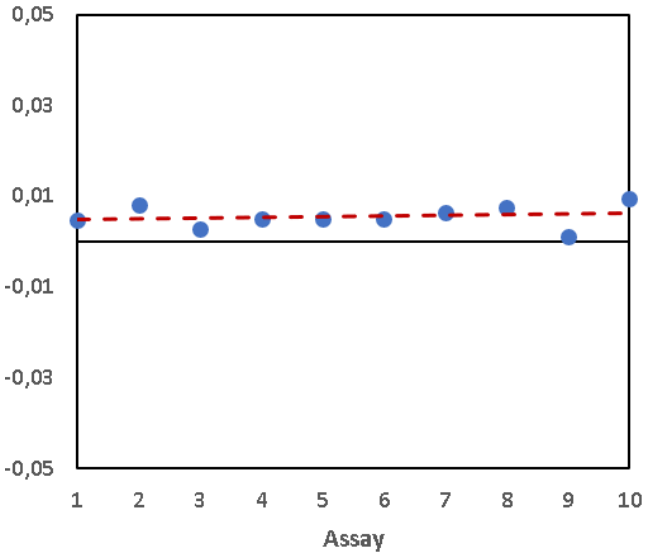

Figure 7: Comparation between the **a** constant of different assays, with aqueous solution flow rate constant.

$$d(x) = ax^2 + (\omega - a)x + 15(\omega - 2a) + c1 \qquad (1)$$

with $\omega = \frac{b1-c1}{b2-c2}$.

A similar experiment was done with the dispersed phase 9. In this case, for each assay the flow rate of

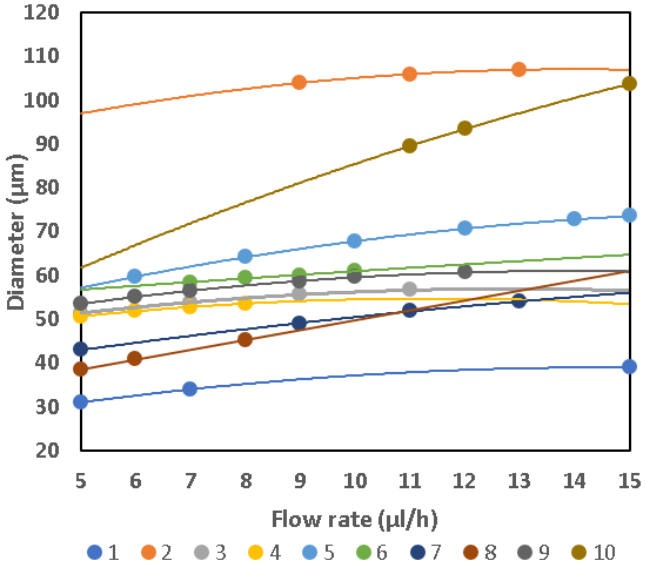

Figure 8: Droplet diameter versus flow rate of the aqueous solution, for a constant continuous phase flow rate.

continuous phase has a constant value, meanwhile the flow rate of the dispersed phase is varying along the assays.

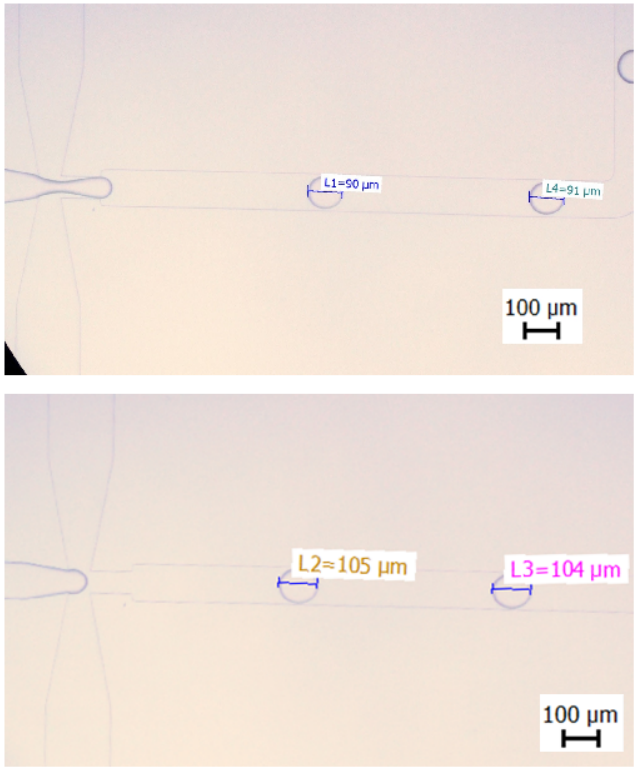

Figure 9: Images of droplet formation for different aqueous phase flow rates. The total aqueous phase was kept at 60 μl/h. While the solution assumes values of 11 μl/h (top left), 12 μl/h (top right) and 15 μl/h (bottom)

.

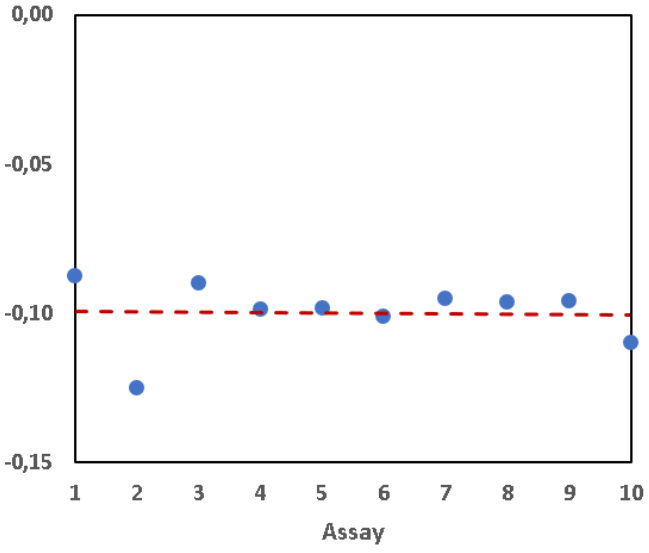

Figure 10: Comparation between the **a** constant of different assays, with oil flow rate constant.

In this case, the increase of particle diameter is between 0,5 and 4% for each increment of 1μl/h in the flow, depending on the initial flow of the dispersed phase (Figure 8). And as with oil, a quadratic regression was performed for each of the tests. From these assays, the constant **a** was obtained and compared (Figure 10).

The value of **a** oscillates around ≈-0,10.

3.2. Size along the chip

Besides the flow focusing, there are other key points along the microchip. Points like the wavy channels for extraction of water, continuous phase II input to the device and wavy channels for cross-linking of alginate droplets (gelation) were also compared, for a constant flow rate of all inputs phases.

As it is possible to see in Figure 11, the particle size decreases along the microchip, specially after the two wavy channel. It is caused because of the diffusion of some water particles into continuous phase and the cross-linking and gelation. Between the flow focusing junction and the end of the diffusion channel, in average, the particles decrease 12%. Meanwhile between the end of diffusion channel and the end of gelation channel the is a decreasing of 6% on the size of the particle.

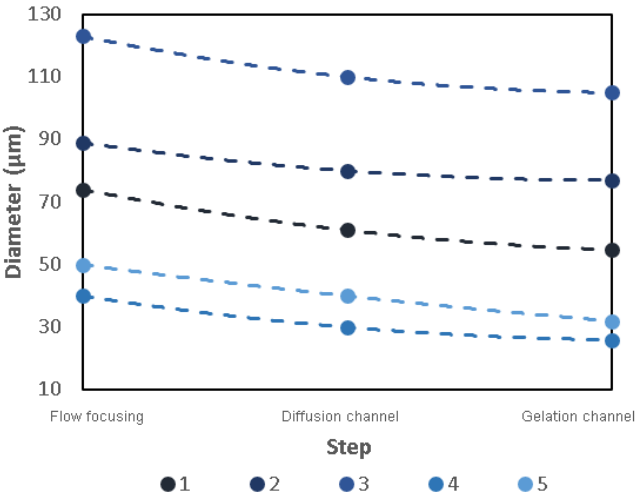

Figure 11: Graphic showing the decreasing of the size for different steps into the microchip, for different assays. The step 1 is after the continuous phase I addition in the flow focusing part, the step 2 is after the diffusion of water in the first wavy channel and the step 3 is after the cross-linking with Ca+ and diffusion of water in the second wavy channel.

of the alginate by addition of calcium ions, leading to the formation of solid alginate microparticles.

The Figure 11, shows the variation of the size of the particles along the microchips. As is possible to see, there is a progressive decreasing depending of in which step the particle is measured.

In some cases, at points of velocity increasing of the continuous phase, such as in the flow focusing junction or during the input of continuous phase II, the particles can get flatter, acquiring more elliptical shape than

spherical. Visually, the particles seem to have a different shape than before the increasing of the flow rate. In the first case, in the first case, the continuous phase flow goes from null to significantly higher. In the second case, the flow of the continuous phase is the sum of the oil flow and oil with added calcium iodide.

3.3. Surface modification of microparticles

After producing the particles, they are modified for using them as targeted delivery particles, so the effect of particle modification was studied. Chitosan solutions with concentration 1% was tested for different curing times: 15 minutes, 1 hour and 6 hours (Figure 12).

Figure 12: Pictures of particles under influence of a magnetic field.

The modification is done in acetic acid solution environment. The average diameter of the particles prepared had decreased significantly.

From 15 min to 1h there is a decreasing of 17% in the size of the particle and 27% from 1h to 6h.

3.4. Effect of iron oxide

The particles obtained with coated iron oxide have potential in medicine, particularly as magneto-responsive drug delivery carriers. It is possible to control the movement of magnetic particles in the biological object by external magnetic field. In addition, iron oxide nanoparticles can be used as a local source heat in the presence of an alternating magnetic field in the radio frequency band.

During the modification, the iron oxide used in the preparation of the alginate solution gives an advantage when handling them. due to easy and faster decantation.

Figure 13: Pictures of particles under influence of a magnetic field.

The alienation of the particles are a response of the particles to the magnetic fields since it is energetically favorable (Figure 13). In the corrugated configuration, the magnetic field is concentrated in the aggregation of particles. They are more easily magnetized than the aqueous medium, this lowers the magnetic energy.

3.5. Model Analysis

The particle diameters obtained experimentally were compared with the simulation in COMSOL Multiphysics, for the same flow rate of the continuous and dispersed phase (Figure 14).

The error between the simulation and the values obtained experimentally are $\leq$7% (Table 2). The influence of the continuous phase flow rate changing can be also compared. The flow of alginate was kept constant at 5 μl/h, while the flow of oil was changed for each simulation.

Table 2: Table comparing the diameter of the particles obtained experimentally and using COMSOL Multiphysics.

Assay	Simulated diameter (μm)	Experimental diameter(μm)	Error(%)
1	67	69	2.9
2	49	52	6.1
3	40	41	2.5

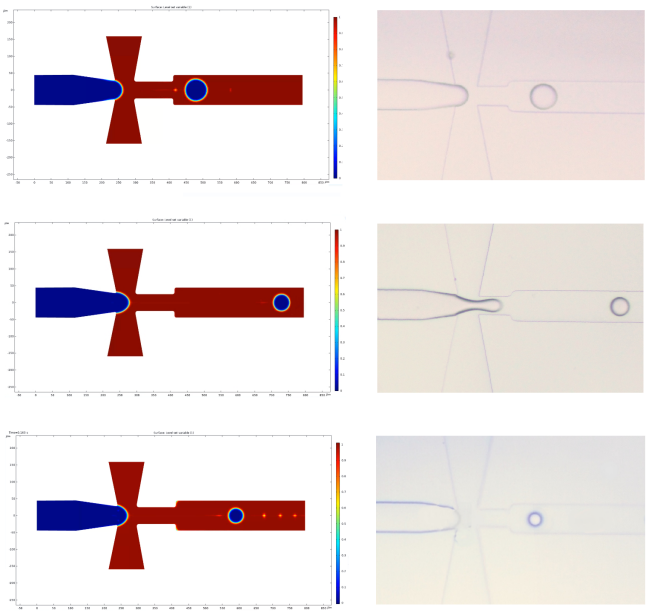

Figure 14: Comparison between simulated and experimental particles for values of flow rates of continuous and dispersed phase of 70 and 7 μl/h (assay 1, top), 120 and 5 μl/h (assay 2, middle), 150 and 5μl/h (assay 3, bottom), respectively.

From the Figure 15 is possible to obtain decreasing percentage of the diameter of the particles per 10 μl/h increase of the flow continuous flow rate and compare it with the values obtained experimentally. They vary

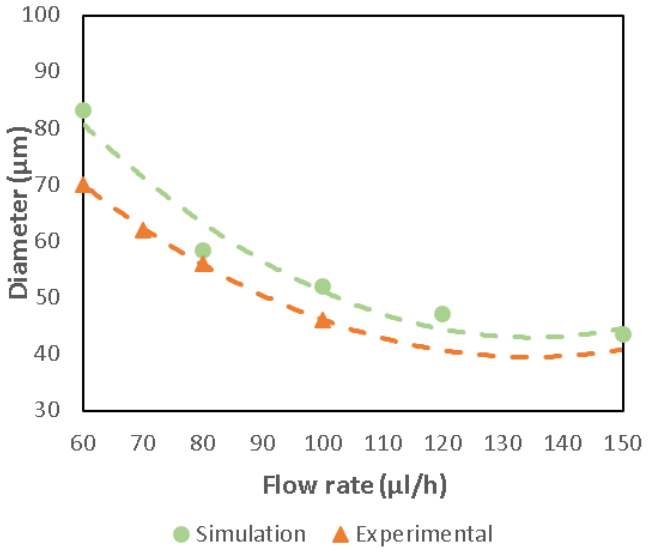

Figure 15: Comparison of the size of the particles produced for different flow rate of continuous phase.

between 4,1% and 14% depending of the flow. The constant **a** was also obtained from the simulation in order to predict the six of the particles obtained for higher and lower flow rates. The constant **a** have a value of 0,0068, 18% lower than the value obtained experimentally (Table 4).

Table 3: Comparison between the percentage of variation and the value of **a** for experimental assay and simulation.

	Variation per 10μl/h (%)	Value of **a**
Experimental	4,8-15	0,0056
Simulation	4,1-14	0,0068

The influence of oil flow rate was also studied in the COMSOL simulation (Figure 16).

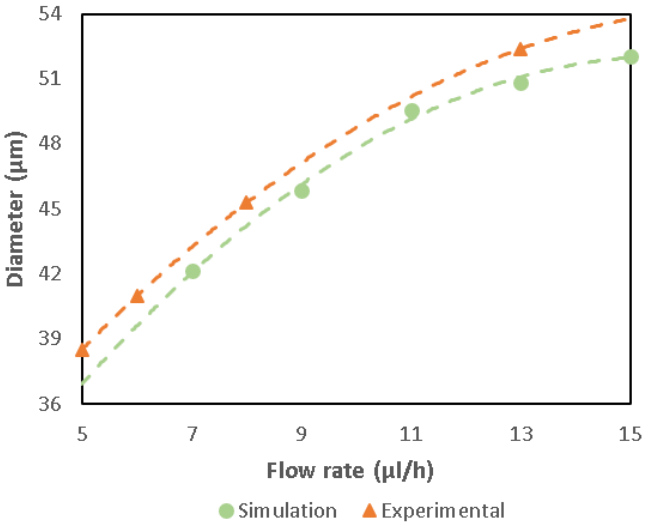

Figure 16: Comparison of the size of the particles produced for different flow rate of dispersed phase.

As the previous simulation, the value of the size change percentage was obtained as well as the value of **a**. The particles diameter decrease between 1,2% to 4,4% for each 1 μl/h increasing of the dispersed flow rate and the value of **a** is -0,12, 16% lower than the value obtained experimentally (Table 4).

Table 4: Comparison between the percentage of variation and the value of **a** for experimental assay and simulation, for alginate flow rate increasing.

	Variation per 1μl/h (%)	Value of **a**
Experimental	1,2-4,4	-0,10
Simulation	0,5-4,0	-0,12

4. Conclusion

The field of microfluidics has made tremendous strides in recent years with the majority of the effort focused on chemical analysis. Microfluidic devices are in many respects ideally suited to this task because they can be made at low costs relative to traditional instrumentation and are small and thus potentially quite portable.

The extractive gelation process was used for downscaling the droplet volume produced in a flow-focusing cross junction, and on-chip gelation with subsequent magnetic separation of the produced gel microparticles was employed as a separation and purification method.

First, microchips of PDMS microchips were fabricated using two ways of assembly of the parts of the microchip: taking advantage of the heat surface before total polymerization and using plasma surface activation. The easy assembly of microchip makes such tips suitable for versatile tests of chip prototypes. The robust nickel mould has been found useful in the numerous fabrications of PDMS microstructures.

The particles and microparticles, consisting of alginate and iron oxide nanoparticles, were prepared in different flow rates. The rate of variation of the particles was studied increasing the flow rates of the continuous phase or the dispersed phase. A second degree trend line was modeled to each set o values, from which parameter **a** of the polynomial equation was obtained. As well as the rate of increasing or decreasing of the particles, depending on the flow rate of alginate solution (0,025% w/w) with iron oxide (c=5,6 mg/mL) and 1-undecanol with 5% w/w of surfactant ABIL.

The particle sizes were also compared for each position in the microchips, especially at points of increase or decrease in speed. From these values, the rate of decrease of the particle was obtained. Either after the addition of 1-undecanol with ABIL, in which water diffuses into the oil, as after the addition of 1-undecanol with ABIL and CaI (2% w/w).

Later, the microchip shape designed in Corel Draw was loaded to the simulation software COMSOL Multiphysics and a simulation of the flow focusing cross junction was done. It is the one of the most important point of the microchip since from this point will depend the size and shape that the particle will adopt along the microchip. Through this simulation, several simulations were made to compare these values with the values obtained experimentally: the rate of variation of the diameter of the particle and the constant **a** of the trend line.

References

[1] Fluigent, "Microfluidics definitions and advantages." `https://www.fluigent.com/microfluidic-expertise/what-is-microfluidic/microfluidic-definitions-and-advantages/`, last accessed on 2020-12-09.

[2] C. J. L. B. L. G. H. M. U. C. N. Bruce K. Gale, Alexander R. Jafek and S. K. Kamarapu, "A Review of Current Methods in Microfluidic Device Fabrication and Future Commercialization Prospects," *Microfluidics and Nanofluidics*, vol. 3, no. 60, 2018.

[3] G. M. Whitesides, "The origins and the future of microfluidics," *INSIGHT OVERVIEW*, vol. 442, 20106.